RUSSIAN JOURNAL OF EARTH SCIENCES, VOL. 3, NO. 6, PAGES 395–404, DECEMBER 2001

Migration of the Azores superplume: Geophysical and petrologic evidence

L. V. Dmitriev[1], S. Yu. Sokolov[2], and N. S. Sokolov[3]

[1]Vernadsky Institute of Geochemistry and Analytical Chemistry, Russian Academy of Sciences (GEOKhI)
[2]Geological Institute, Russian Academy of Sciences
[3]Lomonosov State University, Moscow

Abstract. A detailed study of the best understood portion of the Mid-Atlantic Ridge (MAR) between 0° and 80°N latitude, which involved a comparison of petrologic and geochemical parameters of magmatism against satellite altimetry, seismology, deep tomography, and geoid surface data, reveals a persistent correlation of these parameters along the MAR's zero-age axial zone. In this zone, coexistence of plume- and spreading-related basaltic associations (PB and SB, respectively), originating in two fundamentally contrasting geodynamic settings, has been shown to occur. The way these associations are distributed within the ridge is in accordance with its tectono-magmatic segmentation and corresponds to the correlation of petrologic and geophysical parameters. Results thus obtained provided an incentive to reconstruct the tectono-magmatic conditions of genesis of the Atlantic lithosphere through time using along-isochron gravity variations overlain on magnetic lineations. It was at this angle that we approached the portion of the Atlantic between 15°N and 40°N latitude. Here, the PB/SB boundary runs near 30°N along the MAR, which corresponds to the south terminus of the Azores megaplume. Along the M5, M13, M21, and M30 (west and east) magnetic lineation pairs after [*Sandwell and Smith,* 1997], isochron profiles of free-air gravity anomalies were constructed with a 2′ resolution. A detailed correlation of isochron profile pairs with the along–ridge axis profile bears the following implications: (1) The lithospheric tract between the Kane and Atlantis fracture zones has been generated over the past 65 m.y. in a steady spreading environment virtually outside the reach of any tectonic or magmatic overprint. (2) Regions corresponding to PB and SB provinces within the study area have existed since at least 67 Ma. (3) Symmetry perturbations in the gravity field on both sides of the ridge axis induced by subsequent magmatic or tectonic events cannot be timed using paleomagnetic data. (4) As suming that the correlation of petrologic and geophysical parameters, which has been ascertained for zero-age events along the MAR axis, has been maintained since 67 Ma, it can be inferred that over this time interval the geodynamic setting responsible for the formative conditions of the Azores megaplume migrated southward from 41°N to 30°N latitude at a rate of ca. 18 mm/yr.

Introduction

Among burning, albeit unresolved, problems of ocean-floor geology one faces the issue of mantle magmatism evolving during the formation of oceanic lithosphere from the initial continental breakup to lithospheric accretion in present-day mid-ocean ridges (MORs). Direct and reliable evidence

Paper number TJE01076.
ISSN: 1681–1208 (online)

The online version of this paper was published December 27, 2001.
URL: http://rjes.agu.org/v03/tje01076/tje01076.htm

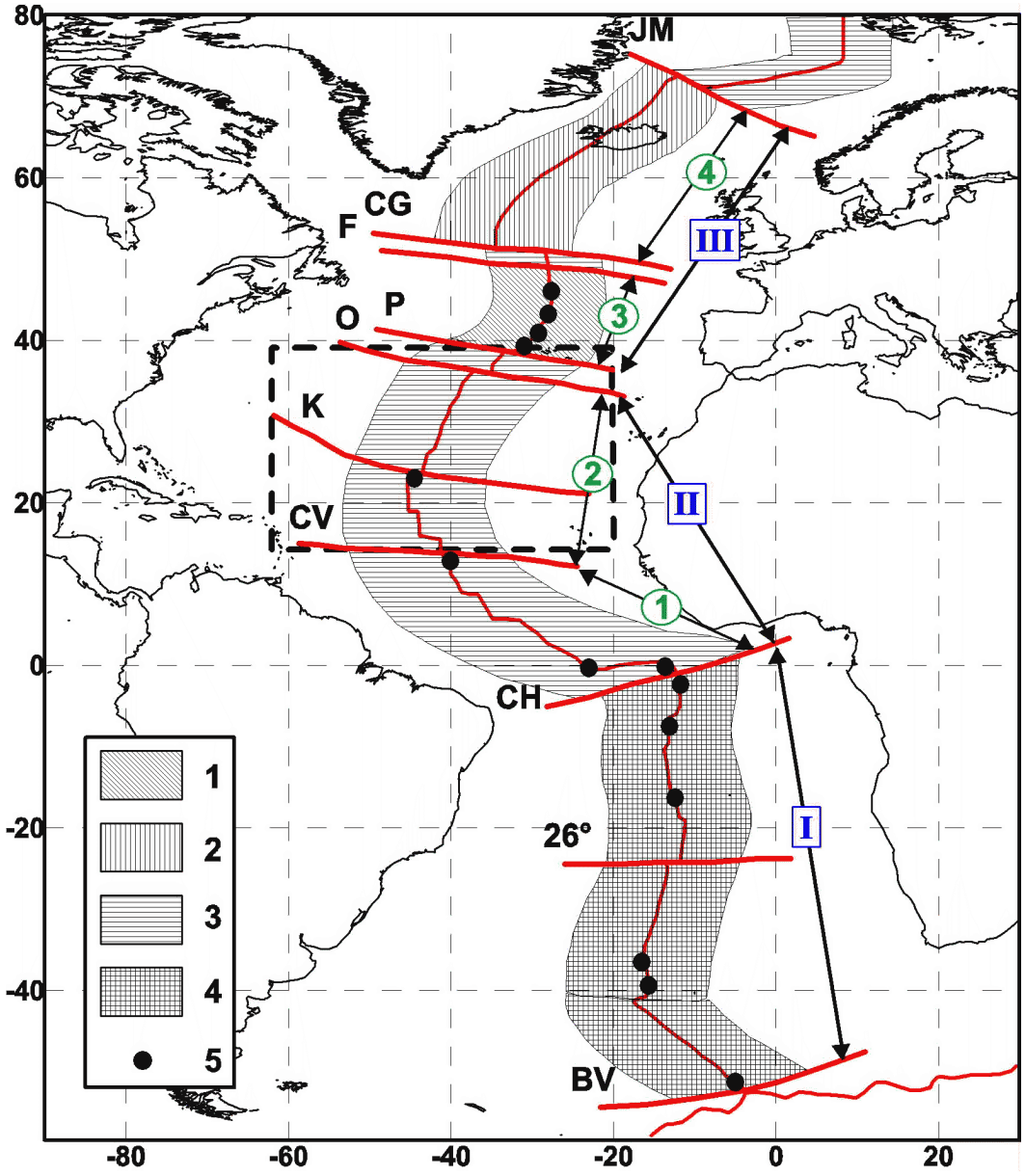

Figure 1. Scheme showing tectono-magmatic segmentation of the Mid-Atlantic Ridge, supplemented after [*Dmitriev,* 1998]. Symbols: 1 – ORT 1; 2 – ORT 1 + ORT-Fe ; 3 – ORT 2; 4 – ORT 1 + ORT 2; 5 – ORT-K. For ORT 1, ORT 2, etc., see explanations in text. The plume association includes ORT 1, ORT-Fe, and ORT-K; the spreading association is represented by ORT 2. I, II, and III – 1st order segments: I = South Atlantic, II = southern North Atlantic, III = northern North Atlantic. (1)–(4) – 2nd order segments: (1) – subequatorial segment, (2) – central segment, (3) – Azores segment, and (4) – Iceland segment. Fracture zones: JM = Jan Mayen, CG = Charlie Gibbs, P = Pico, O = Oceanographer, K = Kane, CV = Cape Verde, CH = Chain, 26° = 26°S lat. FZ, BV = Bouvet. Study area outlined by dashed line.

on magmatism is only available from axial and crestal MOR portions, i.e., it portrays events no farther back than ca. 1 Ma. Deciphering these events from petrologic and geochemical data points to global and local heterogeneities in mantle sources of basalts, variations in the scale of mantle upwelling and magmatic productivity, etc. These data are indispensable to the statistical quantification of geodynamic settings in which oceanic lithosphere is generated. Sampling coverage of magmatic rocks up to 5–10 m.y. old along outer MOR flanks is rather sparse, and the only evidence on compositions of oceanic basement rocks as old as 150–180 m.y. is that recovered by deep-sea drilling. Judging from these

scanty data, abyssal basalts are similar in their compositional range to MORBs. This affords the sole, albeit crucial, conclusion that, on a global scale, throughout the formation time of the oceanic lithosphere, geodynamic conditions of mantle magmatism have generally remained within the range established for the modern MOR structures. This evidence, however, is clearly insufficient to form a judgment on how magmatism and geodynamics evolved through time and space.

This issue can be approached by correlating data on magmatic petrology, tectonics, topography, and geophysical fields of one or another feature or region, etc. For MORs, such correlations have been documented on a qualitative level in many recent publications.

Lately, high resolution data from geophysical fields in the oceans have become available, and new raw data on MOR magmatism have been amassed. This affords a quantification of the correlation between petrologic and geophysical parameters for the zero-age phase of MOR evolution. A quantification like this was carried out over the best understood northern part of the Mid-Atlantic Ridge [*Dmitriev et al.,* 1999]. The latter study established a persistent correlation between the principal parameters of mantle magmatism, tectono-magmatic segmentation of the ridge, anomalous gravity field, the geoid surface, seismicity, and tomography data. This correlation was viewed as resulting from the interplay of processes of various levels, such as mantle upwelling, tectonics, and magmatism, involved in the formation of MORs, accessible to observation now and not yet obscured by imminent geological events.

Another finding from that study is that mantle magmatism occurs here in two geodynamic settings, clearly distinct in space, sharply contrasting, and linked with independently generated spreading- and plume-related basalt associations. These associations are identified reliably based on major-element variations in basalts. The above provided an incentive for us to venture a reconstruction of how petrologic parameters of ocean floor magmatism have been evolving through time, based on gravity variations along magnetic lineations of various ages, and assuming the correlation between these values to remain essentially unchanged over time. This study sets out to attempt such a reconstruction.

Choosing a Study Area

To ensure a trustworthy solution to the problem posed, we had to choose a limited area in the North Atlantic whose formation was least affected by tectonism and magmatic overprint, but which included plume- and spreading-related basalt associations along the MAR's strike. Another critical condition was for magnetic lineations in this area to be distributed as uniformly as possible. These requirements were met by the area between 14°N and 39°N, which is outlined in Figure 1, showing a scheme of tectono-magmatic segmentation of the MAR, modified after [*Dmitriev,* 1998]. According to this scheme, the selected area is located within the southern region of the North Atlantic (first-order Segment II) and occupies the entire central segment of this region (second-order Segment 2). This scheme is substantiated in detail in the work just referred to, and we will thus mention only those considerations prerequisite to further constructions:

(1) The selected segment is the most ancient fragment of the Atlantic lithosphere (opening time of ca. 170 Ma).

(2) The entire period of formation of this segment was controlled by steady slow spreading, whose rate remained virtually constant (ca. 3 mm/yr.).

(3) The area is least affected by faulting. The number of transform faults per unit area is considerably smaller here compared to other segments of the Atlantic. Offsets along these transforms are smaller as well.

(4) The central part of the area (the EW-trending zone between 20°N and 35°N) is virtually free of the impact of subsequent magmatic processes. Intraplate magmatic manifestations are pronounced clearly only near the boundaries of the area.

(5) Most part of the MAR, from the Cape Verde FZ at 15°N to 30°N, is composed of spreading-related basalts. The Azores superplume is centered at ca. 45°N, outside the study area. Transition from the spreading association to plume association occurs between 30°N and 40°N, i.e., within the selected segment.

A general idea of the bathymetry of the chosen area is provided by the map constructed on predicted topography data [*Smith and Sandwell,* 1997], presented in Figure 2. The figure shows that the greater part of the area has a smooth topography, shallowing gradually from abyssal ocean floor to the ridge's axial part. Along the strike of the ridge, the relief rises smoothly from 30°N northward. Figure 3 presents a gravity field map at the same scale based on satellite altimetry data with a 2′ resolution [*Sandwell and Smith,* 1997]. A map showing distribution of identified magnetic lineation axes in the study area, constructed after [*Cande et al.,* 1993], is given in Figure 4. It shows clearly that lineations as old as ca. 70 m.y. are distinct throughout their length. It is also apparent that spacing between the lineations is consistent enough on both sides of the ridge axis. Given a distribution pattern of magnetic lineations as uniform as this, along-isochron profiles can be constructed quite confidently.

Characteristics of Magmatism and the Correlation of Petrologic Data with the Geophysical Fields

As mentioned above, in currently forming MORs, mantle magmatism is taking place in two fundamentally dissimilar, plume- and spreading-related, geodynamic settings. Detailed petrologic and geochemical characteristics of the MOR magmatism and the underlying causes of the correlation between geodynamic settings and specific basalt associations being generated are addressed in [*Dmitriev,* 1998; *Dmitriev et al.,* 1999]. Here, our concern is only with the information needed to solve the problem posed.

The plume basalt association is generated during intense upwelling of mantle material from depths between 400 to 700 km or more, possibly including the lower mantle, and

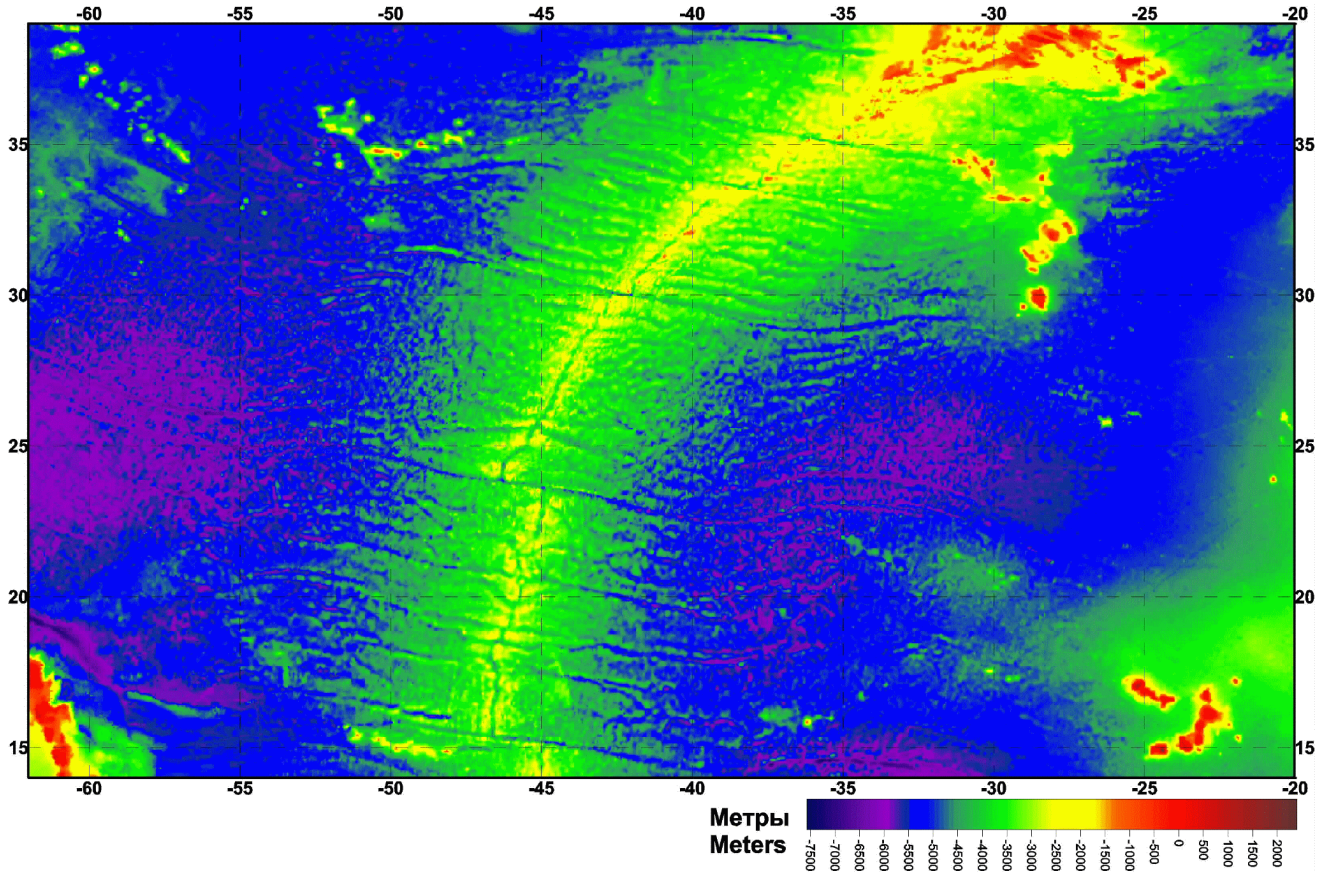

Figure 2. Bathymetric chart of the study area, after [*Smith and Sandwell,* 1997].

its partial melting at elevated (over 1400°C) temperatures with the resultant basaltic magmatism. This association includes three ORT (ocean rift tholeiite basalt) groups: The ORT 1, the most widespread group, whose parental melts segregate from mantle sources at relatively high PT parameters. Geochemically, most of these basalts are classed with the N-MORB type of [*Wilson,* 1989], showing a slight enrichment. The ORT-Fe group is comprised of Fe-enriched basalts derived through in-chamber differentiation of ORT 1. The rare ORT-K group includes basalts generated at the greatest depths and highest temperatures. These basalts are considerably enriched geochemically and correspond to the T-MORB type of [*Wilson,* 1989]. The development of the plume association involves voluminous volcanism and the formation of a basaltic layer of increased thickness and of positive topographic forms.

The spreading basalt association is generated through slow upwelling of mantle material from relatively shallow, less than 400 km, depths. Its parental melts originate at temperatures below 1400°C. The spreading association is typified by small volumes of volcanism and a thin to absent basaltic layer. The association includes the most widespread group of depleted basalts, ORT 2 (N-MORB), and the ORT-Na group, the less widely spread variety of the most depleted ORT 2 with elevated Na abundances.

The plume and spreading basalt associations are identified reliably enough based on their chilled glass compositions using the 8-component discriminant D1, whose value depends on PT parameters of the formation of parental melts and of their evolution. Increased spreading rates result in a greater magmatic productivity, an expanded range of PT parameters of cotectic crystallization and ORT compositions, and a greater proportion of spreading to plume basalt associations.

At low spreading rates, plume development occurs as an independent process superimposed on spreading. Plume- and spreading-related ORT associations are then distinctly apart in space. In the North Atlantic, this is demonstrated spectacularly by how sharply the Iceland and Azores superplumes, as well as microplumes south of the Cape Verde FZ, at 22°N and 25°N, are delimited. With increasing spreading rates, boundaries between plume and spreading associations are erased.

An example of correlation of petrologic parameters (the pressure of cotectic crystallization of a basaltic melt, the discriminant D1, and basaltic crust thickness calculated as a function of volcanic productivity) and geophysical fields (the geoid surface and free-air and Bouguer anomalies) throughout the MAR length from the equator to 80°N is given in Figure 5 after [*Dmitriev et al.,* 1999]. The same work shows that the distribution of petrologic parameters reflecting the development of magmatism agrees well with the along-MAR tectono-magmatic segmentation, seismicity, heat flow, and

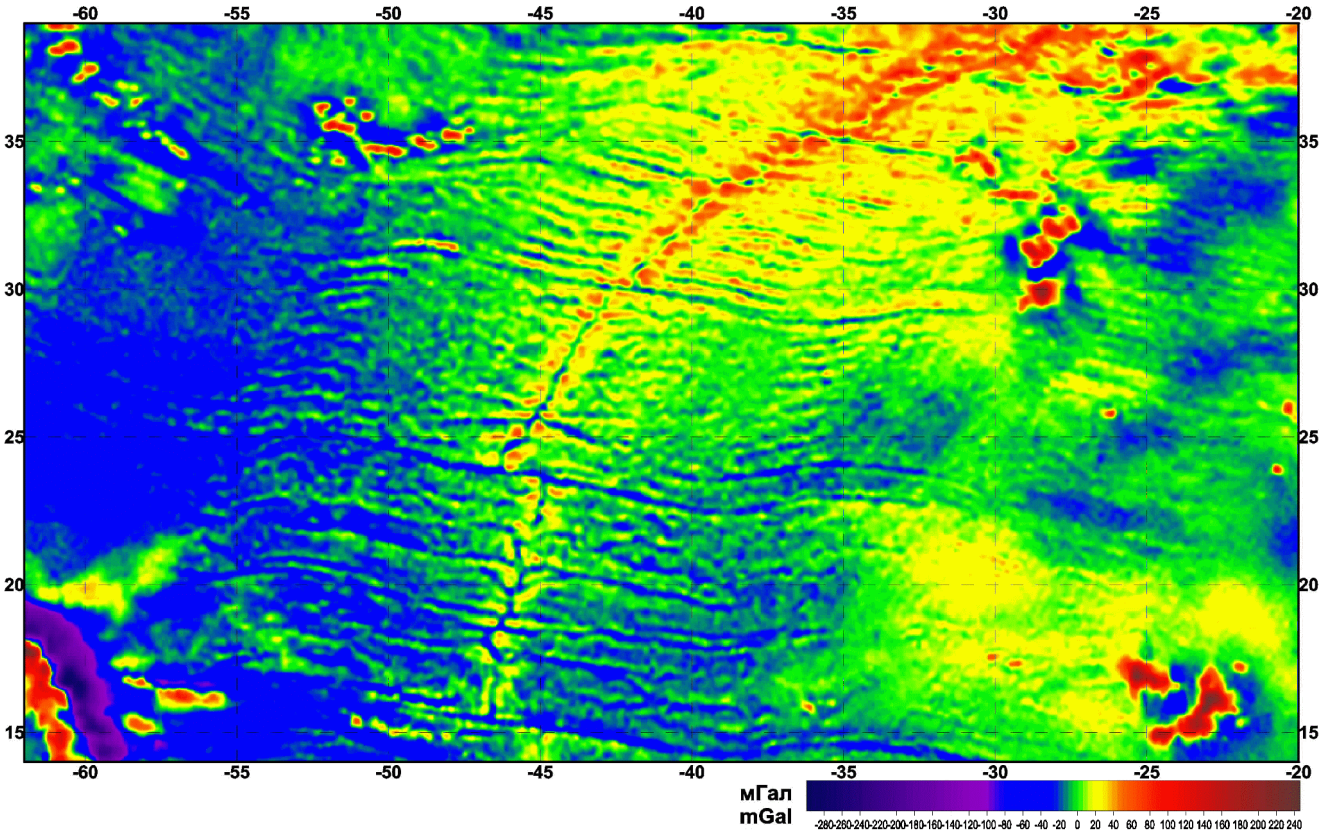

Figure 3. Map showing distribution of free-air gravity anomalies in the study area from satellite altimetry data [*Sandwell and Smith,* 1997].

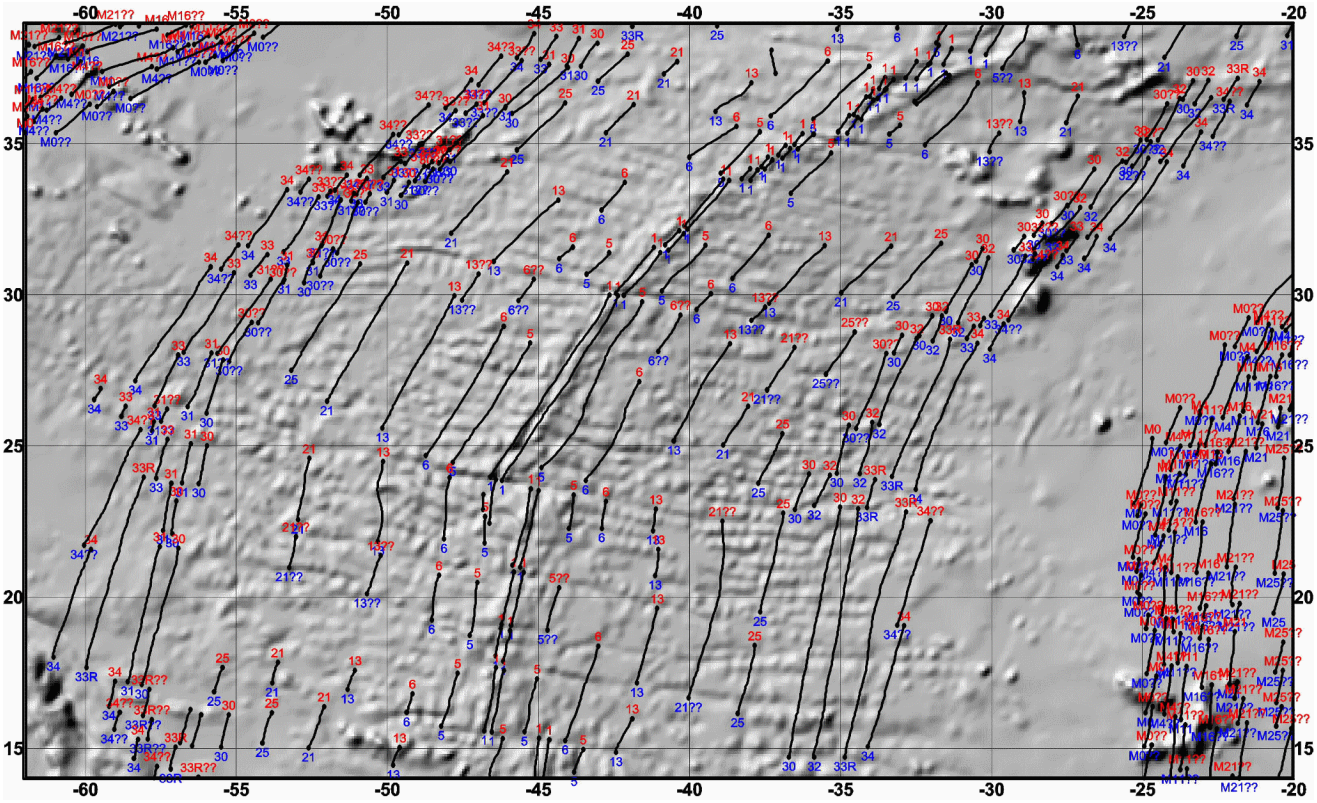

Figure 4. Location of tagged magnetic lineations in the study area, after [*Cande et al,* 1993].

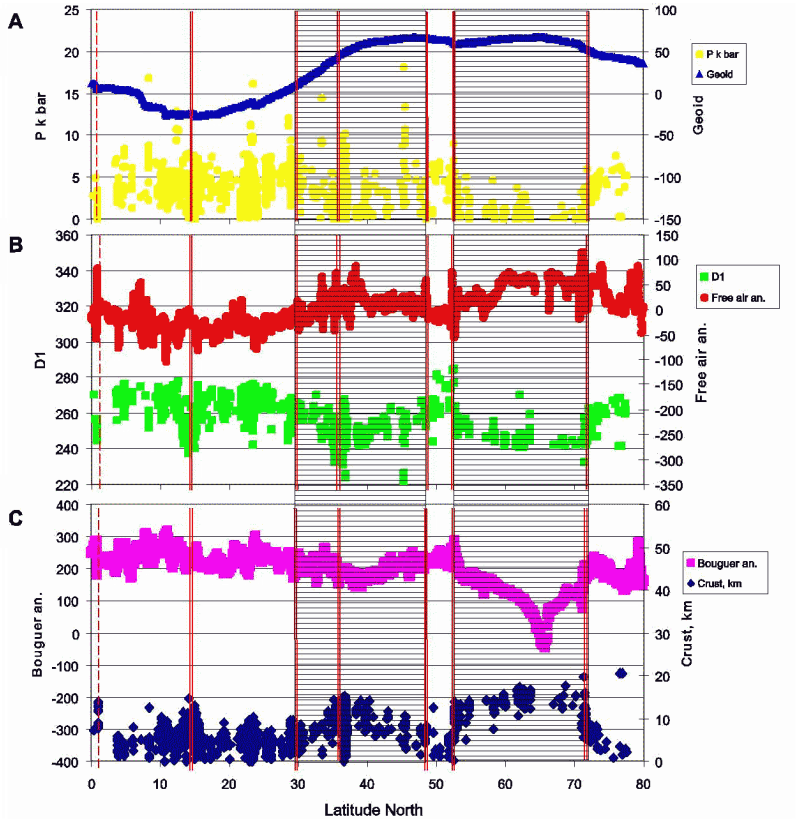

Figure 5. Correlation of geophysical and petrologic parameters along the MAR axial zone from the equator to 80°N latitude. Vertical lines, fault boundaries between ridge segments (Figure 4). Plume association regions shaded. (a) Geoid surface after [*Lemoine et al.,* 1996] and pressure of cotectic crystallization of the ORT; P, kbars. (b) Free-air gravity anomalies [*Sandwell and Smith,* 1997] and the parameter D1. (c) Bouguer anomaly and basaltic crust thickness (see text).

seismic tomography data. As mentioned above, the correlation of all the parameters in point with geologic and geophysical characteristics of the MAR is due to an intimate interplay of all the geologic processes involved in the formation of present-day oceanic lithosphere in the MAR on a regional scale.

Examples of the correlation of petrologic and geophysical parameters along the MAR axis within the chosen region are shown in Figures 6 and 7. Figure 6 exhibits clearly an inverse correlation of the discriminant D1 and free-air anomaly values, which actually reflect topographic features. A negative correlation of Bouguer anomalies, portraying crustal density distribution, and calculated basaltic layer thickness, or volcanic productivity, is shown in Figure 7.

Reconstructing Petrologic Parameters from Free-air Anomalies

Solving the problem posed included two stages.

(1) Constructing isochron profiles along the ridge axis (zero-age profiles) and along the magnetic lineation pairs, M5 (9.5 Ma), M13 (35.5 Ma), M21 (46.5 Ma), and M30 (67 Ma) using the scale of [*Cande and Kent,* 1992] on both sides of the ridge. These profiles, drawn on a shaded relief map based on [*ETOPO5,* 1993] data, are shown in Figure 8. The same map depicts the occurrence of plume and spreading basalt associations outside the MAR using the GEOKhI data base.

(2) Along these profiles, free-air anomaly values shown in Figure 9 were restored. Here, horizontal lines correspond to zero anomaly. Positive values are coded red.

Figure 9 reveals the following characteristics of the free-air anomalous pattern in the study area:

(1) Along the axial rift zone, the general transition from negative to positive free-air anomalies, in terms of means rather than individual spikes, begins north of 30°N. This is also the area of transition from spreading to plume basalt associations, the south terminus of the Azores megaplume (see above).

(2) Transition from negative to positive values in a S–N direction occurs along each pair of isochron profiles, with elevated anomalous values forming a symmetric V-shaped pattern: along M5, on both sides of the ridge, transition

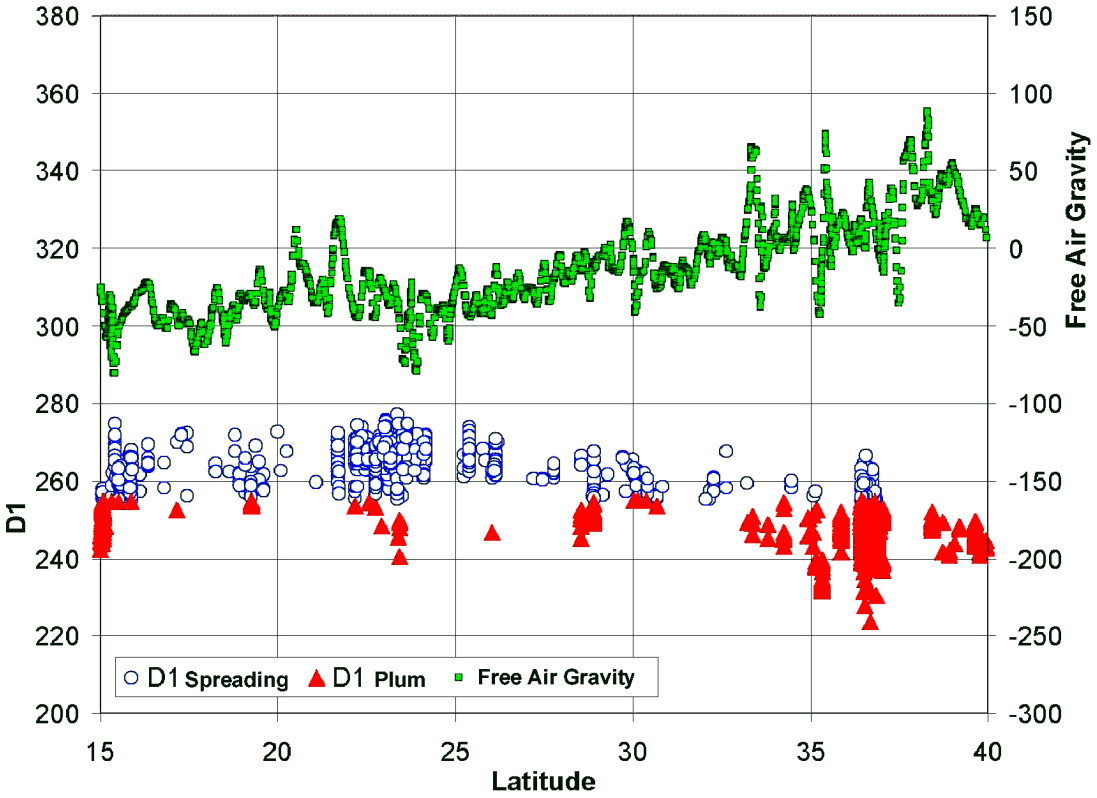

Figure 6. Correlation of free-air anomaly and the discriminant D1 along the MAR axis in the study area. D1 computed from a sample of 2964 chilled glass analyses from the GEOKhI data base, including Volcanic Deep Sea Glass Data Base, W. G. Melson et al., Smithsonian Institution, Department of Mineral Sciences. 2000; Ridge Petrological Data Base, Lamont Doherty Earth Observatory, 2000, new and published data. Distributions of plume and spreading basalt associations shown by different symbols.

to positive values occurs near 23°N, and along M13, at ca. 30°N. A similar pattern is displayed by the western M21 and M30 lineations, their positive values migrating gradually northward as their age increases. With the eastern M21 and M30 lineations, this pattern is upset, because their negative values give way to positive ones further south here, at 25°N and 28°N, respectively. The V-pattern just mentioned of negative vales giving way to positive ones is perturbed in the MAR axial zone. This is due to the fact that the magnitude of free-air gravity anomalies is affected by the overall topographic level, chiefly determined by the degree of lithospheric cooling away from the MAR axis. Introducing due corrections to the magnitude of free-air anomalies from profile to profile would eliminate the differences in mean background values on the profiles in the segment under study without affecting the position of the V-pattern formed by dissimilar anomalous values along the profiles. For this reason, no corrections were calculated.

(3) The smoothest gravity field with the most symmetric distribution along isochron profile pairs is maintained between 20°N and 30°N, or, roughly, between the Kane and Atlantis fracture zones.

Discussion

Assuming that the correlation of zero-age petrologic and geophysical parameters has persisted throughout the lithosphere formation time in the study region (see above), the increase in free-air anomaly values can be inferred to mark the transition from spreading-to plume-related basalt associations. Hence, the northward widening V-shaped pattern of positive anomalies might be due to the plume having gradually migrated over the past 67 m.y. from north to south in the course of formation of the region's lithosphere.

Upset gravity field symmetry in the northeast part of the region, along the eastern profiles 21 and 30, might be due to a local volcanic overprint giving rise to the Atlantis–Meteor seamount system. Complications in the free-air anomaly pattern in the southwest part of the region might also be due to superimposed geologic processes, related in this case to the formation of features such as the roughly EW-trending Royal Trough on the MAR's west flank.

By and large, data presented here are not at variance with the known concepts of plume formation scenarios and

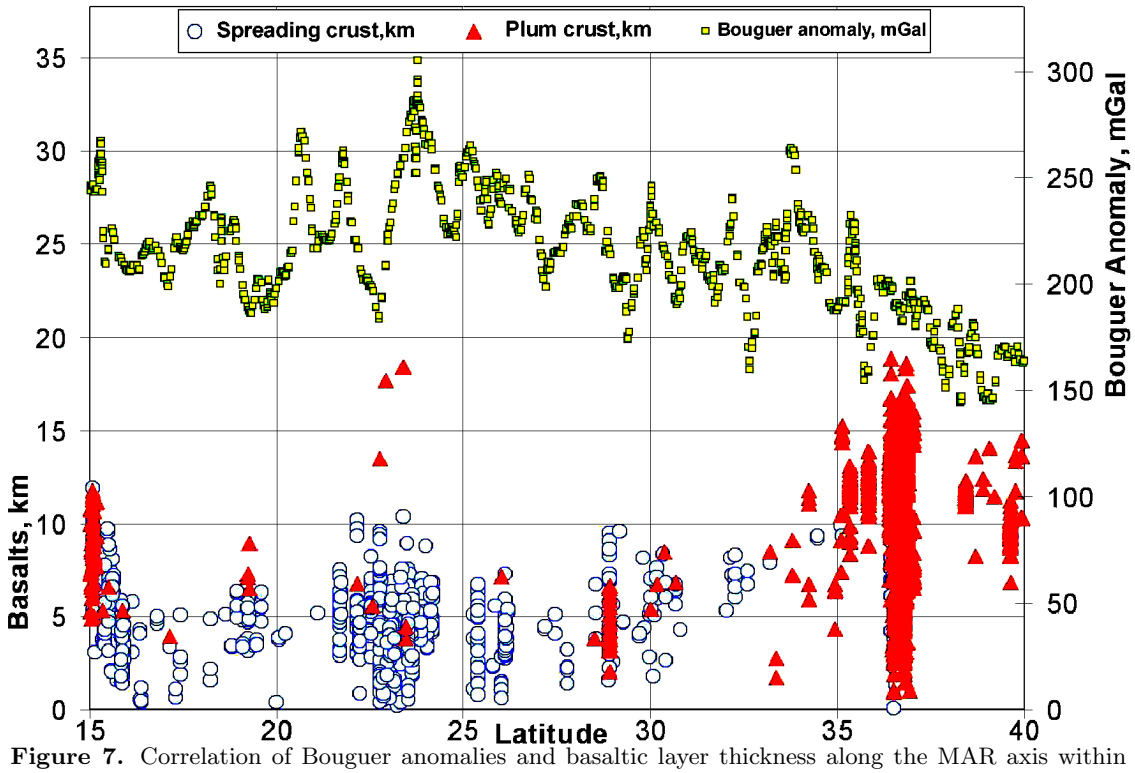

Figure 7. Correlation of Bouguer anomalies and basaltic layer thickness along the MAR axis within the study area. Basaltic layer thickness computed from the same sample using the parameter $Na_{(8)}$ [*Klein and Langmuir,* 1987]. Distributions of plume and spreading basalt associations shown by different symbols.

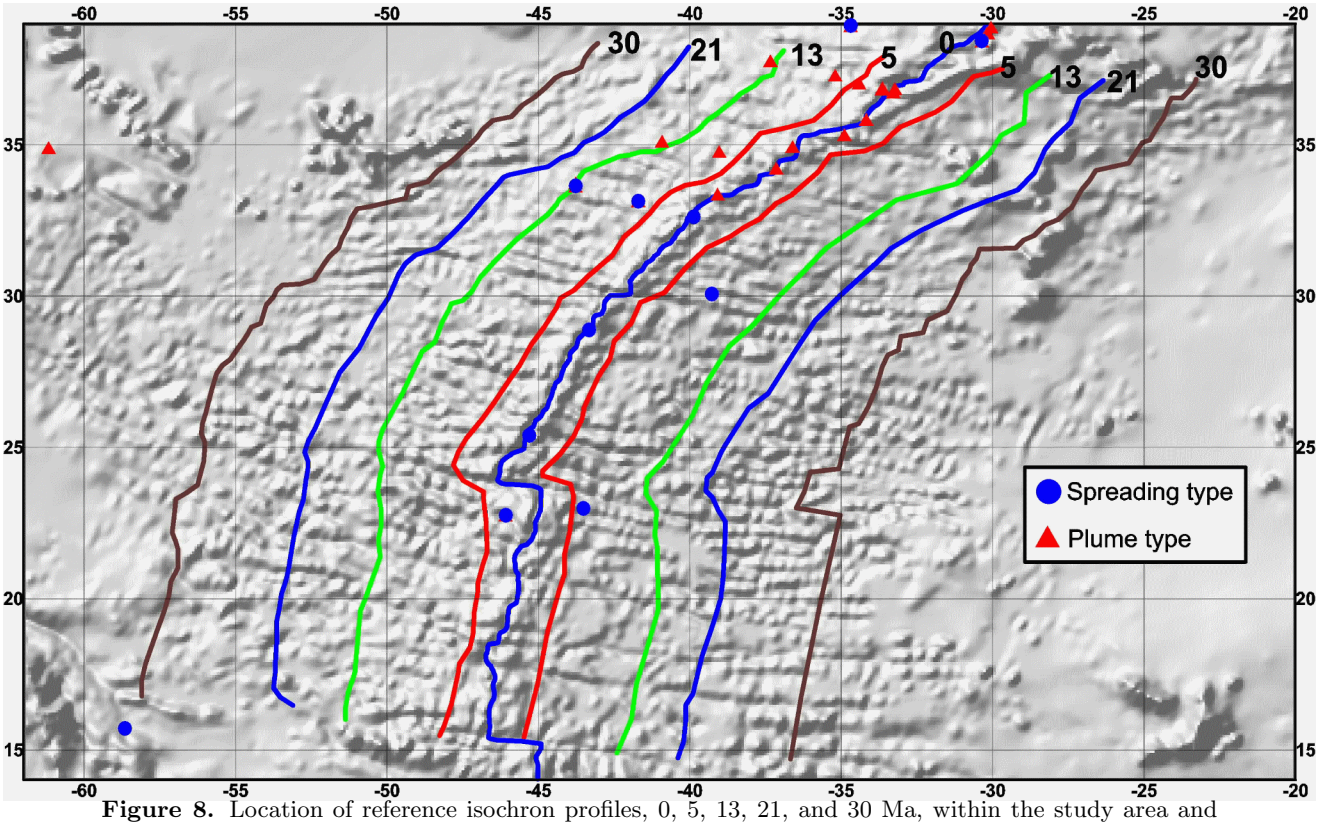

Figure 8. Location of reference isochron profiles, 0, 5, 13, 21, and 30 Ma, within the study area and distribution of plume and spreading basalts recovered outside the MAR zone.

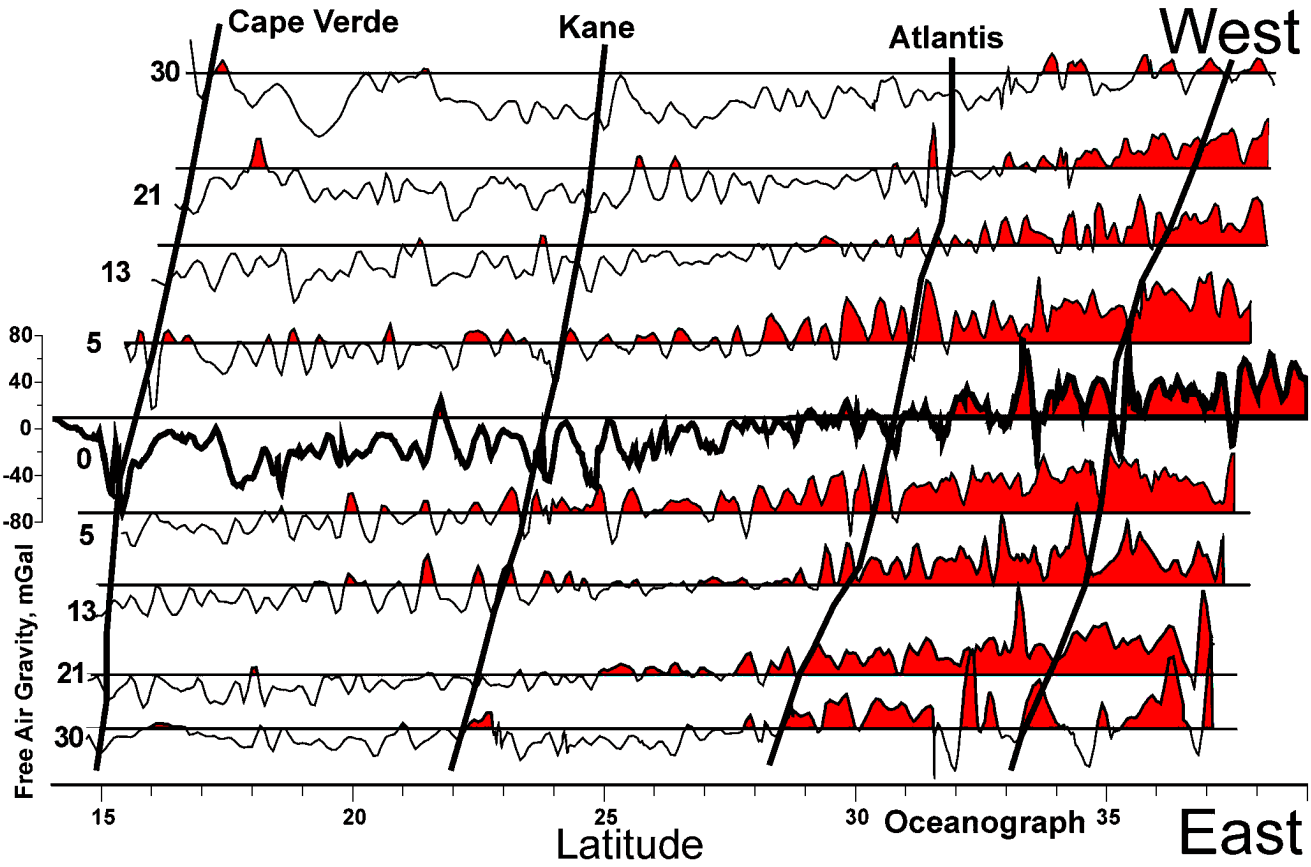

Figure 9. Distribution of free-air anomaly values along the MAR axis and along the 0, 5, 13, 21, and 30 Ma isochron profile pairs. Positive anomaly values coded red.

plume–spreading interaction in the mid-ocean ridge system, of migrating plumes, and of results of this process, as recorded in the petrologic parameters of magmatism and in the geophysical and geomorphologic lithospheric signatures; e.g., [*Grachev,* 1987; *Ito and Lin,* 1995; *Ribe et al.,* 1995; *Schilling,* 1991; *Sleep,* 1996; *Vogt,* 1976; *White et al.,* 1995; *Yale and Phipps Morgan,* 1998]. A study of the latest 10 m.y. migration of the Azores megaplume, drawing on a detailed correlation of the MAR morphology, tectonics, gravity field, tomography, and magnetic versus bathymetric data between 36°N and 40°N on the one hand and petrologic modeling data on the other, is presented in [*Cannat et al.,* 1999]. According to this study, the Azores megaplume has been migrating at 60 mm/yr for several million years. If it is taken for a proved fact that the V-shaped pattern of free-air anomalies under discussion results from a plume magmatism zone migrating southward throughout the Cenozoic, then the angle of inclination of this V-pattern in the space vs. time, or along-MAR distance vs. anomaly age, reference frame yields the average migration rate. Assuming that the plume front, established from the V-shaped pattern of free-air anomalies, has migrated approximately from the Oceanographer FZ to Kane FZ, i.e., ca. 11°, or 1221 km, since M30 (67 Ma) to the present, we obtain a migration rate of ca. 18 mm/yr, an average value for the Cenozoic. Considering that global tectonic processes on the earth are non-linear, i.e., that they occur in a pulse mode, it can be ascertained with confidence that rates averaged over periods long enough will invariably be lower than peak rates from certain particular epochs. Therefore, the time behavior of the Azores plume, inferred from the totality of extremely diverse data by many researchers, is defined in an internally consistent manner as a non-steady state southward migration involving the formation of structures superimposed on a standard oceanic crust.

Conclusion

Our study shows that, in the course of formation of the Atlantic lithosphere, within the chosen study area the geodynamic setting giving rise to mantle plumes has existed for at least 60 or 70 m.y. The fact that plume-related basalt associations have migrated over this time interval a distance of at least 1200 km here, with spreading rate remaining comparatively steady, implies that plume formation does not depend on spreading and is overprinted on it. This corollary further supports the inference of independence of the two processes, advanced by [*Dmitriev et al.,* 1999].

The new approach here proposed to reconstruct petrologic parameters of magmatism from isochron gravity anomaly profiling data holds promise for solving the issue of magmatic evolution during the formation of oceanic lithosphere through the Earth's history. While exercising this approach, the choice of one or another study area should take due account of a number of constraints imposed by (i) inconsistencies in sampling coverage of magmatic rocks, (ii) nonuniform reliability of magnetic data, and (iii) tectonic histories varying in complexity from area to area. To further refine this approach, one can make use of Bouguer anomalies and heat flow data.

Acknowledgments. Thanks are due to A. F. Grachev, N. V. Koronovsky, S. A. Silantiev, and A. O. Mazarovich for their fruitful discussion of our paper. This work was supported by the Russian Foundation for Basic Research (project no. 01-05-64168) and by the Ministry of Industry, Science, and Technology of the Russian Federation (Key Regions of the Mid-Atlantic Ridge project).

References

Cande, S. C., and D. V. Kent, A new geomagnetic polarity time scale for the Late Cretaceous and Cenozoic, *J. Geophys. Res., 97,* 13,917–13,951, 1992.

Cande, S. C., J. L. LaBrecque, R. L. Larson, W. C. Pitman, III, X. Golovchenko, and W. F. Haxby, Magnetic lineations of World's Ocean basins (map), Amer. Ass. Petrol. Geol., Tulsa. OK. 1989, Digitized Set by G. Cole, Global Relief Data CD. NOAA Product # 1093-A27-001, 1993.

Cannat, M., A. Briais, C. Deplus, J. Escarti, J. Georgen, J. Lin, S. Mercouriev, C. Meyzen, M. Muller, G. Pouliquen, A. Rabain, and P. da Silva, Mid-Atlantic Ridge-Azores hotspot interactions: Along-axis migration of a hotspot-derived event of enhanced magmatism 10 to 4 Ma ago, *Earth Planet. Sci. Lett., 173,* 257–269, 1999.

Dmitriev, L., Variations in basaltic compositions as a function of their formative geodynamic setting (in Russian), *Petrologiya, 6,* (4), 340–362, 1998,

Dmitriev, L., S. Sokolov, V. G. Melson, and T. O'Hearn, Plume- and spreading-related basalt associations and their record in petrologic and geophysical parameters of the northern Mid-Atlantic Ridge (in Russian), *Russian Journal of Earth Sciences, 1,* (6), 1999.

ETOPO5, Global Relief Data CD, NOAA Product # G01093-CDR-A0001, 1993.

Grachev, A. F., Rift zones of the Earth, 286 p., Nedra, Moscow, 1987.

Ito, G., and J. Lin, Oceanic spreading center-hotspot inter-actions: Constraints from along-isochron bathymetric and gravity anomalies, *Geology, 23,* 657–660, 1995.

Klein, E. M., and C. H. Langmuir, Global correlations of ocean ridge basalt chemistry with axial depth and crustal thickness, *J. Geophys. Res., 92,* 8089–8115, 1987.

Lemoine, F. G., et al., The development of the NASA GSFC and DMA Joint Geopotential Model, paper presented at International Symposium on Gravity, Geoid and Marine Geodesy (GraGeoMar96)., Univ. of Tokyo., Tokyo, Japan, Sept. 30–Oct. 5, 1996, Geoid Undulation Grid from EGM96, NASA-NIMA, 1996 (http://cddis.gsfc.nasa.gov/926/egm96/egm96.html).

Melson, W. G., et al., *Volcanic Deep Sea Glass Data Base,* Smithsonian Institution, Department of Mineral Sciences, 2000.

Mueller, R. D., W. R. Roest, J. -Y. Royer, L. M. Gahagan, and J. G. Sclater, Digital age map of the ocean floor, SIO Reference Series 93-30 (ftp://baltica.ucsd.edu/pub/global_age/).

Ribe, N. M., U. R. Christensen, and J. Theissing, The dynamics of plume-ridge interaction, 1: Ridge-centered plumes, *Earth Planet. Sci. Lett., 134,* 155–168, 1995.

Ridge Petrological Data Base, Lamont Doherty Earth Observatory, 2000 (http://petdb.ldeo.columbia.edu).

Sandwell, D. T., and W. H. F. Smith, Marine gravity anomaly from Geosat and ERS-1 satellite altimetry, *J. Geophys. Res., 102,* (B5), 10,039–10,054, 1997 (ftp://topex.ucsd.edu/pub/).

Sandwell, D. T., and W. H. F. Smith, *Marine gravity anomaly from satellite altimetry,* map, Geological Data Center, Scripps Institution of Oceanography, 1995.

Schilling, J. -G., Fluxes and excess temperatures of mantle plumes inferred from their interaction with migrating mid-ocean ridges, *Nature, 352,* 397–403, 1991.

Sleep, N. H., Lateral flow of hot plume material ponded at sublithospheric depths, *J. Geophys. Res., 101,* 28,065–28,083, 1996.

Smith, W. H. F., and D. T. Sandwell, Global seafloor topography from satellite altimetry and ship depth soundings, *Science, Sept. 26, 277,* (5334), 1997 (ftp://topex.ucsd.edu/pub/, http://edcwww.cr.usgs.gov/landdaac/gtopo30/).

Vogt, P. R., Plumes, subaxial pipe flow, and topography along the mid-oceanic ridge, *Earth Planet. Sci. Lett., 29,* 309–325, 1976.

White, R. S., J. W. Bown, and J. R. Smallwood, The temperature of the Iceland plume and origin of outward-propagating V-shaped ridges, *J. Geol. Soc. London, 152,* 1039–1045, 1995.

Wilson, M., *Igneous Petrogenesis,* 463 pp., London Unwin Hyman Dostal, Boston, Sidney, Wellington, 1989.

Yale, M. M., and J. Phipps Morgan, Asthenosphere flow model of hotspot – ridge interactions: a comparison of Iceland and Kerguelen, *Earth Planet. Sci. Lett., 161,* 45–56, 1998.

Zhang, Y. -S., and T. Tanimoto, Ridges, hotspots and their interaction as observed in seismic velocity maps, *Nature, 355,* 45–49, 1992.

(Received December 3, 2001)